Meteorologische Zeitschrift, Vol. **26**, No. 2, 115–125 (published online January 24, 2017)

The climate of the European Alps: Shift of very high resolution Köppen-Geiger climate zones 1800–2100

Franz Rubel[1*], Katharina Brugger[1], Klaus Haslinger[2] and Ingeborg Auer[2]

[1]Institute for Veterinary Public Health, University of Veterinary Medicine Vienna, Austria
[2]Central Institute for Meteorology and Geophysics, Vienna, Austria

(Manuscript received July 25, 2016; in revised form September 8, 2016; accepted October 4, 2016)

Abstract

Although the European Alps are one of the most investigated regions worldwide, maps depicting climate change by means of climate classification are still not-existent. To contribute to this topic, a time series of very high resolution (30 arc-seconds) maps of the well-known Köppen-Geiger climate classification is presented. The maps cover the greater Alpine region located within the geographical domain of 4 to 19 degrees longitude and 43 to 49 degrees latitude. Gridded monthly data were selected to compile climate maps within this region. Observations for the period 1800–2010 were taken from the historical instrumental climatological surface time series of the greater Alpine region, HISTALP. Projected climate data for the period 2011–2100 were taken, as an example, from the Rossby Centre regional atmospheric model RCA4. Temperature fields were spatially disaggregated by applying the observed seasonal cycle of the environmental lapse rate. The main results of this study are, therefore, 366 observed and predicted (two scenarios) very high resolution Köppen-Geiger climate maps of the greater Alpine region covering the period 1800–2100. Digital data, as well as animated maps, showing the shift of the climate zones are provided on the following website http://koeppen-geiger.vu-wien.ac.at. Furthermore, the relationship between the Köppen-Geiger climate classification and the altitudinal belts of the Alps is demonstrated by calculating the boundaries of the climate zones, i.e. the deciduous forest line, the mixed forest line, the forest and tree line (timber line) and the snow line. The mean altitude of the potential timber line in the greater Alpine region, for example, was calculated to be 1730 m by the end of the 19th century, 1880 m by the end of the 20th century and to lie between 2120 and 2820 m by the end of the 21st century. The latter altitudes were projected for the greenhouse gas scenarios RCP 2.6 (best case) and RCP 8.5 (worst case). The altitude of the timber line (and the other boundaries of the altitudinal belts) is generally higher in the Western Alps, showing a clear west-east slope.

Keywords: HISTALP, COSMO-CLM, representative concentration pathways, altitudinal belts, timber line

1 Introduction

The European Alps are one of the most investigated regions worldwide with respect to climate, climate change and the impacts of climate change. Examples of this includes a report of precipitation climatology presented by Frei and Schär (1998) and mapped by Schwarb et al. (2000), temperature trends investigated by Böhm et al. (2001) and the recent modelling study of Haslinger et al. (2016) which addressed future drought probabilities. Of general interest is the alpine vegetation which is particularly sensitive to the effects of climate change (Grabherr et al., 1994; Theurillat and Guisan, 2001). Spatio-temporal analysis of altitudinal vegetation shifts, for example, was investigated by Diaz-Varela et al. (2007), while Gottfried et al. (2011) demonstrated the coincidence of the alpine-nival ecotone with the summer snow line. The winter snow line varies considerably under the influence of European temperature fluctuations (Hantel and Hirtl-Wielke, 2007), is located at an average altitude of 640 m and is characterized by an upward shift of approximately 120 m per °C climate warming (Hantel and Maurer, 2011).

Independent of these specific examinations, the scientific community requires a simple method to describe the climate or climate change of a specified region. For this purpose, the Köppen-Geiger climate classification in particular has proved successful. The generic climate classification initially developed by Wladimir Köppen (1846–1940) and Rudolf Geiger (1894–1981) was presented in its most popular version by Köppen (1936) and has today been established as a multidisciplinary standard to characterize the climate of a region (Rubel and Kottek, 2011). Applications of the Köppen-Geiger climate classification include investigations on: (1) the subdivision of study sites according to climates such as for micrometeorological flux measurements (Mizoguchi et al., 2009) or for global river discharge (Santini and di Paola, 2015), (2) the extraction of climate zones to assess vegetation coverage and biomass of temperate deserts (Zhang et al., 2016a) or the definition of the

*Corresponding author: Franz Rubel, Climate Change and Infectious Diseases Group, Institute for Veterinary Public Health, University of Veterinary Medicine Vienna, 1210 Vienna, Austria, e-mail: franz.rubel@vetmeduni.ac.at

DOI 10.1127/metz/2016/0816

Mediterranean region to review post-wildfire soil erosion (Shakesby, 2011), (3) the effect on human thermal comfort by urban street configurations (Rodríguez Algeciras et al., 2016), (4) the effect of particulate air pollution on human mortality in the USA (Zanobetti and Schwartz, 2009), (5) the composition of disease vectors in Europe (Brugger and Rubel, 2013), (6) the habitat characterization of new species in South America (Bellini and Zeppelini, 2008), and numerous other studies.

While historical world maps of Köppen-Geiger climate classification were exclusively available as hand drawn maps, e.g. in its latest version from Geiger (1961), early digital world maps were compiled to verify global climate models (Manabe and Holloway, 1975) and to depict the observed shift of climate zones (Fraedrich et al., 2001). The first digital dataset covering the observational period 1951–2000 was published by Kottek et al. (2006). This dataset is publicly available via the website http://koeppen-geiger.vu-wien.ac.at/ and paved the way for easy access to climate classification in various research fields. Four years later Rubel and Kottek (2010) published a time series of Köppen-Geiger maps depicting the shift of climate zones over the 200-year period 1901–2100. These maps were calculated from monthly temperature fields provided by the Climatic Research Unit (CRU) of the University of East Anglia (Mitchell and Jones, 2005) and precipitation fields provided by the Global Precipitation Climatology Centre (Becker et al., 2013; Schneider et al., 2014) as well as from an ensemble of global climate model predictions. Recently, various authors published similar Köppen-Geiger maps based on model outputs calculated for the Climate Model Intercomparison Project (CMIP) and the Paleo Model Intercomparison Project (PMIP). CMIP maps were presented and discussed, for example, by Feng et al. (2014), PMIP maps by Yoo and Rohli (2016) and Zhang et al. (2016b), while Willmes et al. (2016) developed an open source software to calculate Köppen-Geiger maps from the databases of both projects.

Global climate classifications have also been applied to continental and regional scales, thereby generating valuable information in particular for life sciences. Köppen-Geiger maps, for example, have been published for Australia (Crosbie et al., 2012), Brazil (Alvares et al., 2013), South Africa (Engelbrecht and Engelbrecht, 2014) and China (Chan et al., 2016).

Here, the concept of climate classification is applied to the greater Alpine region to depict the shift of climate zones during the 301-year period 1800–2100. Special emphasis is placed on the spatial resolution of the digital maps which were not only provided as pictures but also as digital data. The latter were urgently required for many scientific applications. At present, researchers may use either digital data available with a spatial resolution of 0.5 degrees or less as provided by the studies discussed above or can calculate their own Köppen-Geiger maps from very high resolution temperature and precipitation fields provided by Hijmans et al. (2005). The latter data are representative for the period 1950–2000 and are provided with a spatial resolution of 30′′ (30 arc-seconds). The goal of this paper is to use the well-documented HISTALP database (Auer et al., 2007), as well as model predictions from EURO-CORDEX (Jacob et al., 2014), both spatially disaggregated, to compile a series of Köppen-Geiger maps. These maps have the same spatial resolution of 30′′ than those of Hijmans et al. (2005), but have been calculated as a 25-year running mean from homogenized time series covering the period 1800–2010 and state-of-the-art regional climate model predictions for the years 2011–2100.

2 Data and method

The greater Alpine region is defined as being located between 4° and 19° geographic longitude and 43° to 49° geographic latitude. Three gridded climate datasets were selected to calculate very high resolution Köppen-Geiger climate maps within this region. The first dataset, the *historical instrumental climatological surface time series of the greater Alpine region*, HISTALP (Auer et al., 2007), comprised temperature fields for the period 1780–2008 and precipitation fields for the period 1800–2010 (http://www.zamg.ac.at/histalp/). For this study, the temperature fields were extended until 2010 with the aim of achieving the joint observational period 1800–2010. Monthly HISTALP temperature fields (Böhm et al., 2001; Chimani et al., 2013) and precipitation fields (Efthymiadis et al., 2006; Chimani et al., 2011) were available on a grid equidistant in geographic latitude and longitude with a spatial resolution of 5′ (around 6.5 km · 9.3 km $\simeq$ 60 km^2). The second dataset, monthly precipitation analyses from Isotta et al. (2014, 2015) based on 5,500 daily rain gauge observations, is used as a reference for the high spatial variability of Alpine precipitation. These precipitation fields cover the major part of the greater Alpine region and were nested into the HISTALP precipitation fields for the reference period 1986–2010. From the latter observed and projected precipitation anomalies were calculated and used as input data for the Köppen-Geiger maps. This procedure considers the high spatial reliability of the reference fields from Isotta et al. (2014) by eliminating the spatial bias of the HISTALP precipitation fields, which were analysed from 557 homogenised time series.

The third dataset was taken from the EURO-CORDEX ensemble (Jacob et al., 2014). It includes a variety of climate predictions from different global and regional climate model combinations, which were run for the predefined greenhouse gas emission scenarios. As the main focus of this research lies on the observed shift of climate zones, only the two most extreme greenhouse gas concentrations for the representative concentration pathways, RCP 2.6 and RCP 8.5

Table 1: Seasonal cycle (Jan–Dec) and annual mean (Ann) of the environmental lapse rate. Mean and 95 % confidence interval were calculated from values of different study sites presented by Rolland (2003) within the greater Alpine region. Units °C/100 m.

Period	Mean ±95 % CI
Jan	0.46 ± 0.03
Feb	0.51 ± 0.03
Mar	0.58 ± 0.02
Apr	0.63 ± 0.02
May	0.64 ± 0.01
Jun	0.65 ± 0.01
Jul	0.65 ± 0.01
Aug	0.65 ± 0.02
Sep	0.61 ± 0.02
Oct	0.56 ± 0.02
Nov	0.51 ± 0.02
Dec	0.46 ± 0.03
Ann	0.57 ± 0.01

Table 2: Köppen-Geiger climates of the greater Alpine region as defined by Kottek et al. (2006). Only the arid steppes BSh and BSk as well as the Mediterranean climates Csa and Csb were classified using a precipitation criterion. All other climates were exclusively defined by temperature.

Key	Main climate	Precipitation criterion	Temperature criterion
BSh	Arid	Steppe	Hot
BSk	Arid	Steppe	Cold
Csa	Warm temperate	Dry summer	Hot summer
Csb	Warm temperate	Dry summer	Warm summer
Cfa	Warm temperate	No dry season	Hot summer
Cfb	Warm temperate	No dry season	Warm summer
Cfc	Warm temperate	No dry season	Cool summer
Dfb	Boreal	No dry season	Warm summer
Dfc	Boreal	No dry season	Cool summer, cold winter
ET	Alpine	–	Tundra
EF	Alpine	–	Frost

(Meinshausen et al., 2011), of a single regional climate model were selected to depict the range of possible future climates. The Rossby Centre regional atmospheric model RCA4 (Samuelsson et al., 2011; Strandberg et al., 2014) with boundary conditions from the EC-Earth model was selected to represent climate projections. These projections cover the period 1971–2100, from which monthly temperature and precipitation fields for the period 2011–2100 were used to complement the HISTALP observations. The RCA4 data, provided with a spatial resolution of 0.11°, were interpolated to the HISTALP grid and adjusted to the observations by calculating anomalies from the 25-year reference period 1986–2010 to eliminate model bias. Thus, the final 301-year time series of temperature and precipitation fields comprised 211 years of monthly observations and 90 years of monthly predictions (the latter for two greenhouse gas emission scenarios).

To avoid undesirable short term fluctuations of the Köppen-Geiger climate classes (Rubel and Kottek, 2010), the classifications were not calculated directly from the 301-year time series (with two different scenarios for the projection), but were applied to the 25-year running mean. This procedure was also applied for the spatial disaggregation (downscaling), in other words to increase the spatial resolution from 5′ to 0.5′ = 30′′ by a factor of ten. The grid areas obtained cover 0.6 km^2, resolve Alpine valleys and fulfil even the requirements of challenging biological applications. The environmental lapse rate was used for the spatial disaggregation of the mean monthly temperature fields. It was calculated from data published by Rolland (2003), who presented lapse rates from 4 sites in the Austrian and Italian Alps (Table 1). The seasonal cycle of these lapse rates depicts a typical maximal temperature decrease of 0.65 °C/100 m during the summer months (June, July, August) and minimum values of 0.46 °C/100 m during the winter months (January, December). The monthly lapse rates were implemented using the 30′′ altitude data GTOPO30 of the U.S. Geological Survey (USGS) provided by the Earth Resources Observation and Science (EROS) center (http://earthexplorer.usgs.gov). Although not applied, the mean annual environmental lapse rate representative for the European Alps was estimated as 0.57 °C/100 m. While the spatial variability of the vertical temperature gradients may be considered as minimal (see the 95 % confidence intervals in Table 1), it is not possible to specify a general precipitation-altitude relationship for the entire region of the European Alps. However, as precipitation plays no – or merely a secondary – role in the Köppen-Geiger climate classification of the altitudinal belts of the Alps (see discussion below), a 5 % precipitation increase per 100 m altitude increase was implemented. This estimate follows the precipitation-altitude relationship for low altitudes presented by Frei and Schär (1998).

The calculation of the Köppen-Geiger climate classification was described in detail by Kottek et al. (2006). On the global scale, 31 climate classes identified by a 3 letter code were defined by Köppen (1936). A total of 11 of these climate classes appear within the model domain of the greater Alpine region and are explained in Table 2. These comprise two arid climates (denoted by the first letter B), five warm temperate climates (C), two boreal climates (D) and the two alpine climates (E). The boreal climate is a synonym for the historically introduced term snow climate and, in a global context, the alpine climates are called polar climates. Additional climates on the global scale comprise the equatorial climates denoted by A and further subdivisions of the arid climate B, the warm temperate climate C and the boreal climate D (Kottek et al., 2006).

The two arid climate classes BSk and BSh characterize arid steppes, which are expected to appear in inner Alpine valleys of a future warmer climate. Moreover, this steppisation is restricted to areas of limited geographical extent and only displayed by the very high

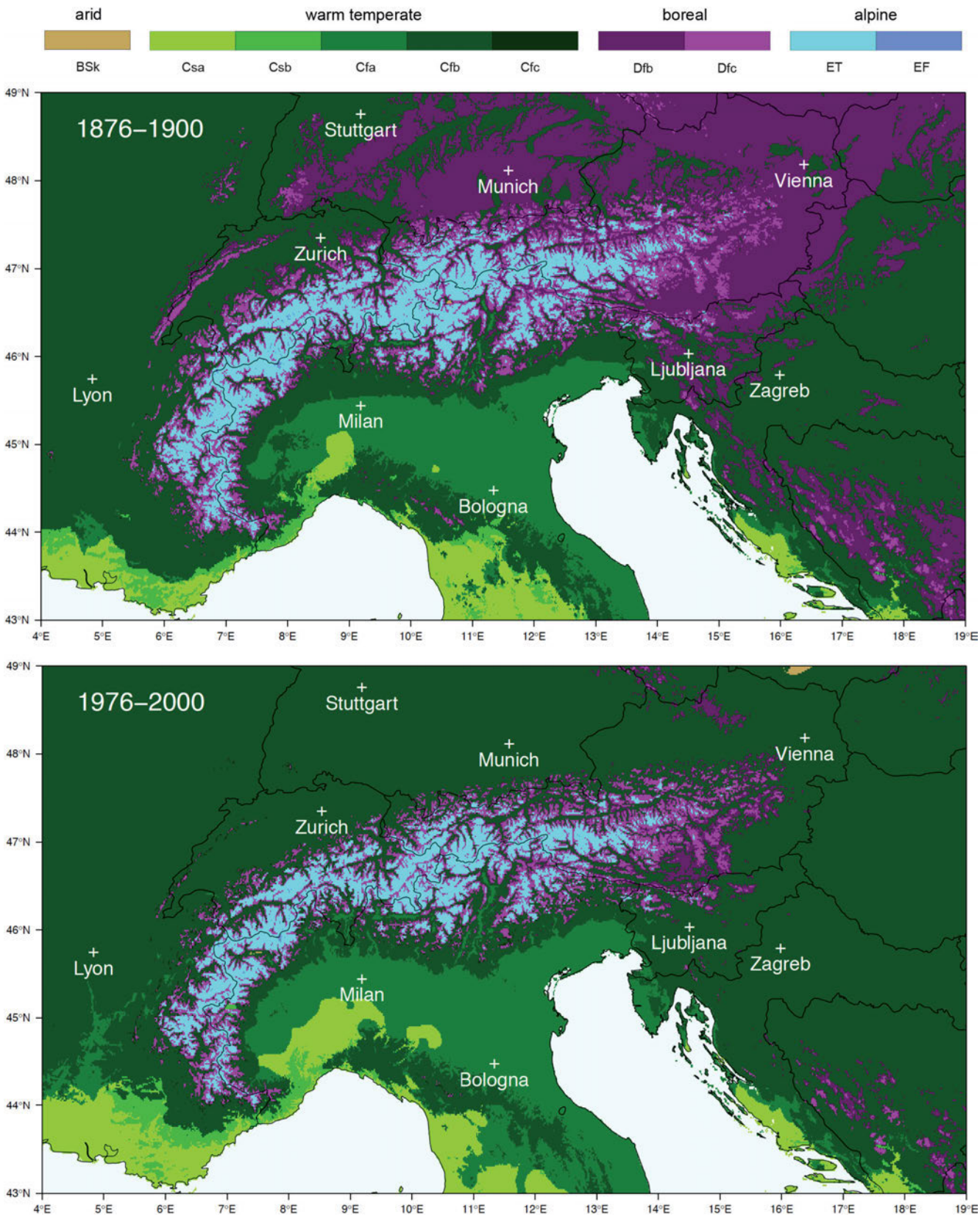

Figure 1: Maps of Köppen-Geiger climate classification for the greater Alpine region calculated from observed temperature and precipitation data. Spatial resolution 30 arc-seconds, data HISTALP, period 1876–1900 (upper panel), period 1976–2000 (lower panel).

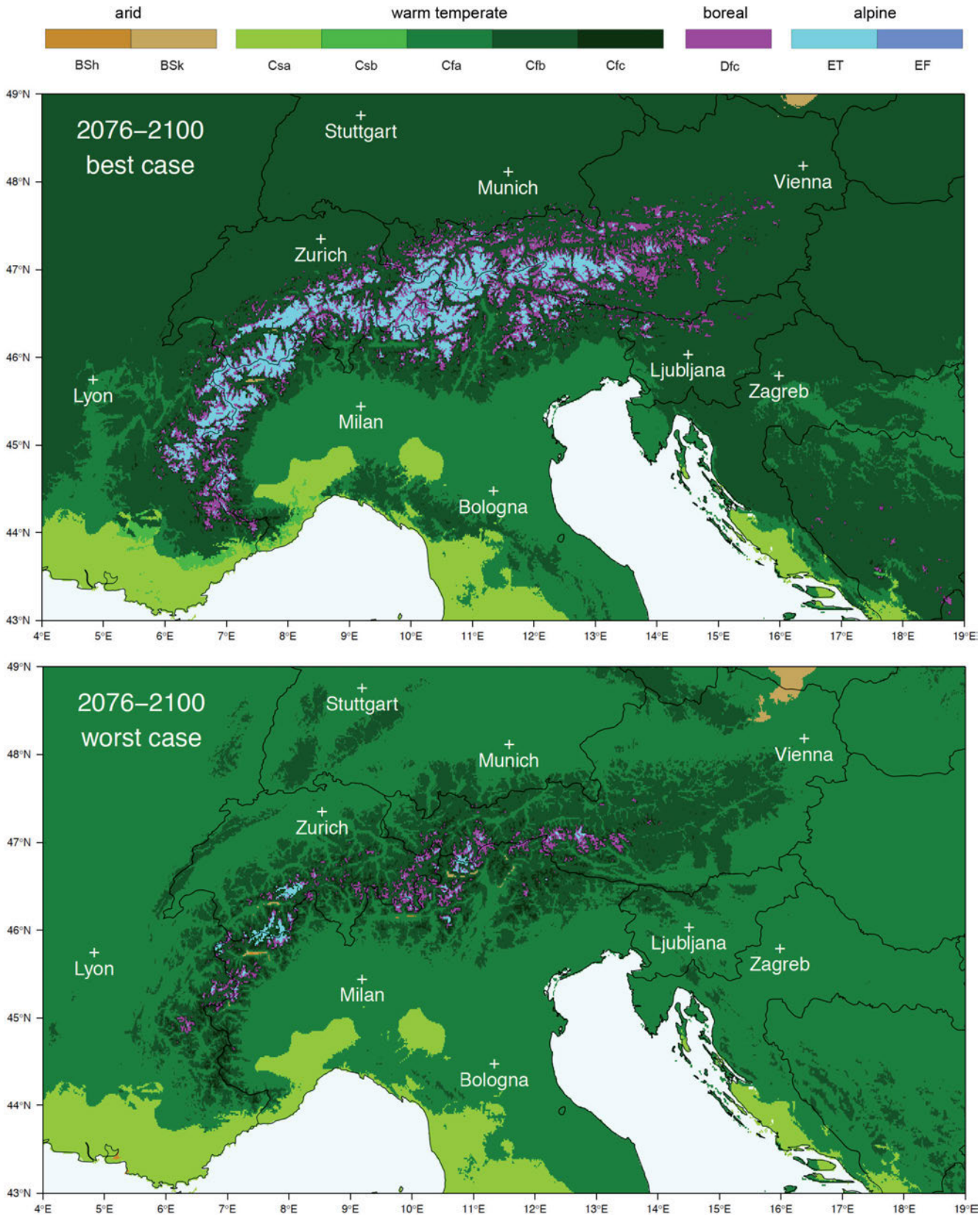

Figure 2: Maps of Köppen-Geiger climate classification for the greater Alpine region calculated from projected temperature and precipitation data. Spatial resolution 30 arc-seconds, period 2076–2100, model RCA4, best case scenario RCP 2.6 (upper panel), worst case scenario RCP 8.5 (lower panel).

resolution of the maps. Much more important are the five warm temperate climates, which cover the main part of the greater Alpine region. Within these climates, a distinction is drawn between the occurrence and absence of a dry season, as well as between cool, warm and hot summers. The Cfb climate (no dry season, warm summers) is the prevailing climate in the north of the Alpine divide. The Cfc climate with cool summers is located in the montane belt of the Alps, whereas the three remaining warm temperate climates were observed south of the Alps. The Cfa climate characterizes a temperate climate with hot summers and no dry season, while the summer dry climates Csa and Csb are sometimes grouped together and are commonly called Mediterranean climate (Shakesby, 2011). The moist boreal climates of the Alps were exclusively classified according to their temperature regime into Dfb (warm summer) and Dfc (cool summer and cold winter). Note that Köppen (1936) developed this classification according to the tree species predominant in different regions under natural conditions. The region of the Cfb climate was predominantly covered with deciduous forest, of which beech were the main tree species. Oak were the predominant species of the Dfb climates and spruce of the Dfc climate. However, over recent decades, beeches and oaks have been replaced by high performance industrial spruce forest. Due to climate change, the economic success of these industrial spruce forests is now in question. Therefore, today's Cfb climate should be interpreted rather as optimal climate for deciduous forest, the Dfb climate as mixed forest climate and the Dfc climate as coniferous forest climate. The timber line separates the cool boreal climate (Dfc) from the alpine tundra climate (ET), where tree growth is no longer possible. The 10 °C isotherm of the warmest month was defined as a criterion. Note that on the scale considered here it is not possible to distinguish between the forest and the tree line. Altitudes above the alpine tundra were covered by the alpine frost (EF) climate. This is located above the 0 °C isotherm, which is an approximation of the snow line.

Thus it becomes immediately evident that the temperature is the essential parameter to classify the Alpine climate according to Köppen (1936). Precipitation plays a minor role. In the present climate, precipitation is used exclusively to define the BSh and BSk climates of dry mountain valleys and to determine the boundary of the Mediterranean climates, i.e. the summer dry climates Csa and Csb. The latter cover coastal regions from sea level up to a height of some 100 meters. The disaggregation of the precipitation fields by applying a precipitation-altitude relationships shows therefore only a minor effect which, however, reflects the general experience. Alternatively, it might be replaced by a simple 2-dimensional spline interpolation.

3 Results

The main results of this study are 366 observed and predicted (two scenarios) very high resolution Köppen-Geiger climate maps for the greater Alpine region covering the period 1800–2100. Both the digital maps, as well as the underlying digital data, are publicly available for further investigations on the website http://koeppen-geiger.vu-wien.ac.at. Fig. 1 depicts two of these maps, one for the 25-year observational period 1876–1900 and one for the more recent observational period 1976–2000. While the years 1876–1900 belong to the coldest years of the entire observational period, the years 1976–2000 illustrate the effect of the recent warming trend. Clearly visible is the strong decline of the boreal climates, which are optimal for coniferous and mixed forests. In the 19th century, the boreal climates Dfb and Dfc covered large areas north of the Alps as well as the Balkans, while they have been pushed back to higher altitudes during recent years. This reduction of the boreal climates becomes more evident when looking at climate projections for the period 2076–2100 (Fig. 2). For both greenhouse gas concentration scenarios, the Dfb climate, i.e. the boreal climate with warm summers, has almost completely disappeared. In contrast, the warm temperate Cfc climate, which was still rare in the 19th century, becomes the typical climate in the montane belt of the Alps. The two greenhouse gas concentration scenarios used result in widely different maps. While the RCP 2.6, hereinafter referred to as, the best case scenario, assumes that the warming trend will not continue during the second half of the 21st century, the RCP 8.5, hereinafter referred to as, the worst case scenario, assumes that the recent trend of increasing temperatures will continue until the year 2100. The projections of the climate zones of both scenarios are far removed from what was observed during the last 200 years. The alpine climates ET and EF will be, in particular, will be forced into small areas in the projection (best case scenario) or will disappear almost entirely (worst case scenario). Assuming the worst case scenario, areas recently classed as the Cfb climate (warm summers) will be covered by the Cfa climate (hot summers) in 2076–2100.

Another way to demonstrate climate change by Köppen-Geiger maps is to observe the boundaries. The most prominent boundary is the mountain timber line. It is not simply a line, but a transition zone between the forest line and the tree line. Note that numerous definitions of the two lines have been given in a variety of studies. Moreover, on a local scale, there are often significant differences between the potential and the current forest and tree lines (Szerencsits, 2012). By means of the Köppen-Geiger climate maps, it is possible to estimate the potential timber line for the entire region of the European Alps. The timber line divides the Dfc climate, naturally covered by coniferous forests, from the alpine tundra climate ET and is exclusively defined by temperature, more precisely by the 10 °C isotherm of the warmest month. As discussed already by Köppen (1919, 1920) and confimed by recent research (Jobbágy and Jackson, 2000), the 10 °C July isotherm is an admissible approximation for the potential timber line in ex-

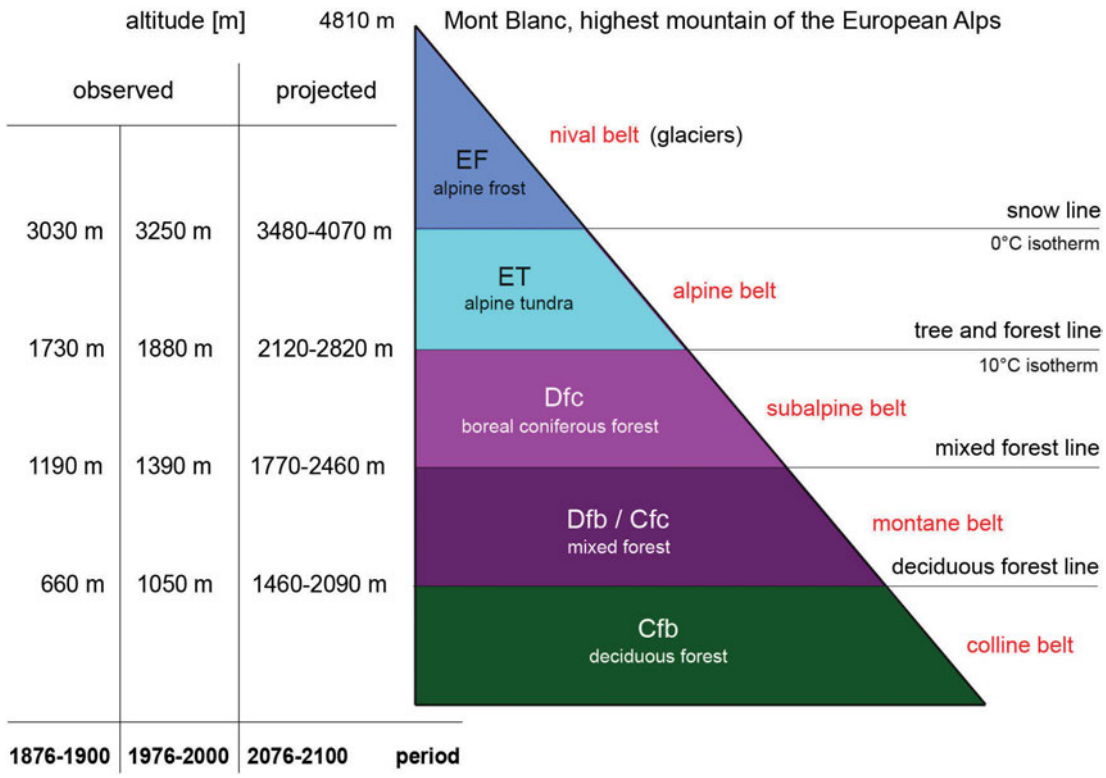

Figure 3: Altitudinal belts of the Alps showing the Köppen-Geiger climate zones together with their boundaries, the deciduous forest line, the mixed forest line, the forest and tree line (timber line) and the snow line. Altitudinal shifts of the lines became visible by comparing the observational periods 1876–1900 and 1976–2000 as well as the two scenario projections for the period 2076–2100. Mean altitudes representative for the greater Alpine region are given. The altitudinal belts of the current climate are comparable to another frequently used, but differently defined classification, which distinguishes between colline, montane, subalpine, alpine and nival belts (red text).

tratropical regions. Note that the 10 °C isotherm of the warmest month, instead of the historically investigated July isotherm, is used as a criterion for the Köppen-Geiger climate classification. The mean timber lines for the greater Alpine region are estimated at altitudes of 1730 m (period 1876–1900), 1880 m (1976–2000), 2120 m (2076–2100, best case scenario) and 2820 m (2076–2100, worst case scenario).

Further boundaries between the Köppen-Geiger climate classes include the snow line (boundary between the alpine tundra ET and the alpine frost EF climate), the mixed forest line (boundary between Dfc and Dfb/Cfc) and the deciduous forest line (boundary between Dfb/Cfc and Cfb). They are related to the altitudinal belts of the Alps. Fig. 3 shows a scheme of these altitudinal belts together with the mean altitudes of the boundaries and the well-known classification according to Ellenberg (Ellenberg and Leuschner, 2010). The latter approximately match the Köppen-Geiger classification of the current climate, although they are defined quite differently. This classification is commonly used in geography, botany, ecology and related sciences. It classifies the altitudinal belts into colline, montane, subalpine, alpine and nival belts. Note that the Ellenberg classification is helpful to understand the relationship between the altitudinal belts and the Köppen-Geiger maps, but does not match the latter for the 19th century, where the boreal Dfb climate covered large areas of the lowlands north of the Alps. The Ellenberg classification also does not concur very well with the Köppen-Geiger maps projected for the 21st century.

A closer look at the observed time series (Fig. 4) shows altitudinal fluctuations of the timber line of approximately more than 100 m within the last 210 years. Minima of 1733 m (period 1809–1833), 1695 m (period 1907–1931) and 1752 m (period 1954–1978) alternate with maxima of 1842 m (period 1852–1876), 1812 m (period 1935–1959) and 1949 m (period 1986–2010). The RCA4 projections, however, do not depict these cyclic fluctuations of around 100 m altitudinal shift per 50 years. They predict a relatively constant warming trend resulting in extraordinarily high altitudes of the timber line. The best case scenario, for example, depicts a maximum altitude of the timber line of 2154 m (period 2044–2068) and, for the worst case scenario, the maximum altitude is projected to reach 2820 m (period 2076–2100). However, it is outside the scope of this study to investigate or discuss whether or not these projections are realistic in view of the fact that observations depict more cyclic trends. The projected Köppen-Geiger maps and the related altitudinal belts of the Alps should be considered as possible realisations of the future provided by the climate modelling community. In contrast, the observed altitudinal belts of the 210 previous years

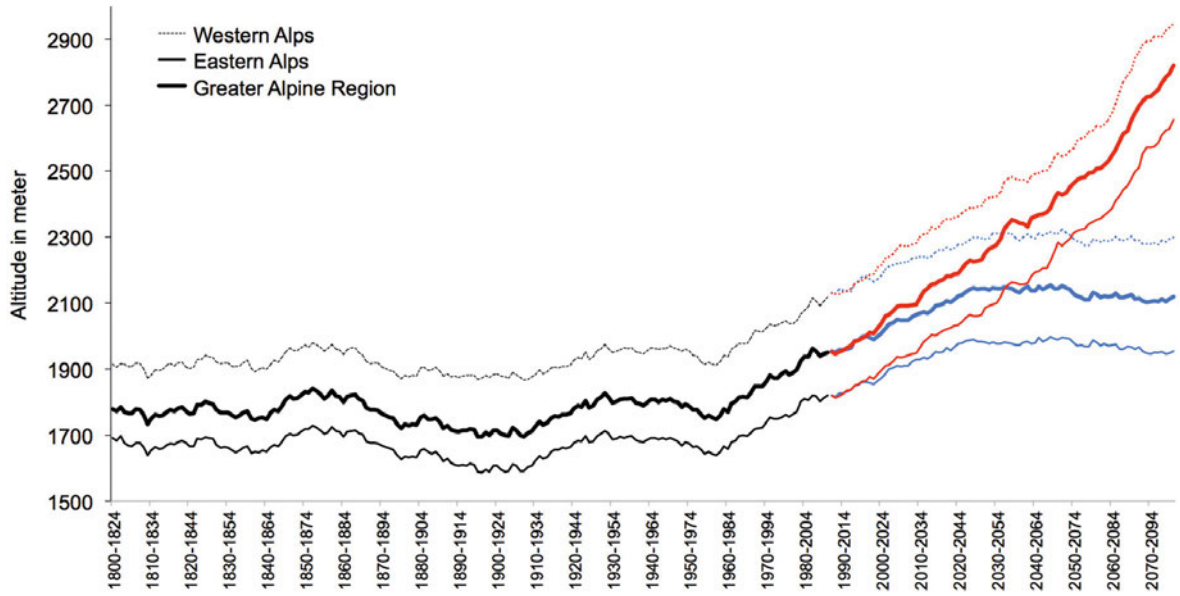

Figure 4: Timber line shift in the greater Alpine region calculated from observed (black), projected best case scenario (blue) and projected worst case scenario (red) Köppen-Geiger maps. Mean value for the greater Alpine region (thick solid), the Western Alps (thin dotted) and the Eastern Alps (thin solid). Moving average over 25 years for the period 1800–2100.

represent a unique database exclusively available for the European Alps (Fig. 3).

4 Discussion and conclusions

Very high resolution Köppen-Geiger climate maps (Fig. 1 and 2) and their relationship with altitudinal belts (Fig. 3) were presented for the greater Alpine region. Although the most comprehensive observational datasets were used, and were combined with the best knowledge available concerning the environmental lapse rate, there is some potential for improvement. Advanced studies on the spatio-temporal variability of the observed and the projected lapse rate, as well as investigations concerning the precipitation-altitude relationships, may improve future Köppen-Geiger climate maps. Furthermore, improvements in the climate projections may be expected from the development of enhanced feedback mechanisms of changing vegetation caused by shifting climate zones.

Here, particular attention was paid to the timber line for which a 301-year time series was presented. When interpreting this time series, it should be noted that the mean altitudes are not comparable with regional altitudes of the timber line. As depicted in Table 3, there are significant regional differences between the Western Alps (5.5°–7.5° W, 44.5°–45.5° N), the Central Alps (9°–11° W, 46°–47° N) and the Eastern Alps (12.5°–14.5° W, 46.5°–47.5° N). The current altitude of the potential timber line in the Western Alps is approximately 280 m above the timber line in the Eastern Alps. Furthermore, from the 19th to the 20th century, the altitude of the tree line has shifted upwards by around 157 m. This upward shift in the Western Alps is 35 m higher than observed in the Eastern Alps. Altitudes of the timber line in the central part of the Alps, however, correspond relatively well with those calculated for the entire greater Alpine region. Similar trends have been estimated for the snow line, as well as the boundaries of the other altitudinal belts (not shown).

Table 3: Altitude of the timber line of the Western, Central and the Eastern Alps for the observational periods 1876–1900 and 1976–2000 as well as for the projection period 2076–2100 (range between best and worst case). Altitudes of the total greater Alpine region (Fig. 3) are given for comparison. Units in m.

Period	1876–1900	1976–2000	2076–2100
West	1880	2040	2300–2950
Central	1790	1920	2110–2780
East	1630	1760	1950–2660
Total	1730	1880	2020–2820

While the 211-year observed time series of climate maps represent a unique dataset, a large variety of model projections may be calculated to represent the future climate. However, even the altitudinal difference between the timber lines in the best and the worst case scenarios, which is approximately 800 m, demonstrates that it is hard to make clear conclusions about the future climate of the Alps. These projections should thus be considered as an example. To investigate additional greenhouse gas scenarios or to apply ensemble predictions as demonstrated on the global scale by Rubel and Kottek (2010) is beyond the scope of this paper. However, recent model validation studies (Kotlarski et al., 2014; Torma et al., 2015) and ensemble prediction studies (Gerstengarbe et al., 2015) provide additional insights into this topic.

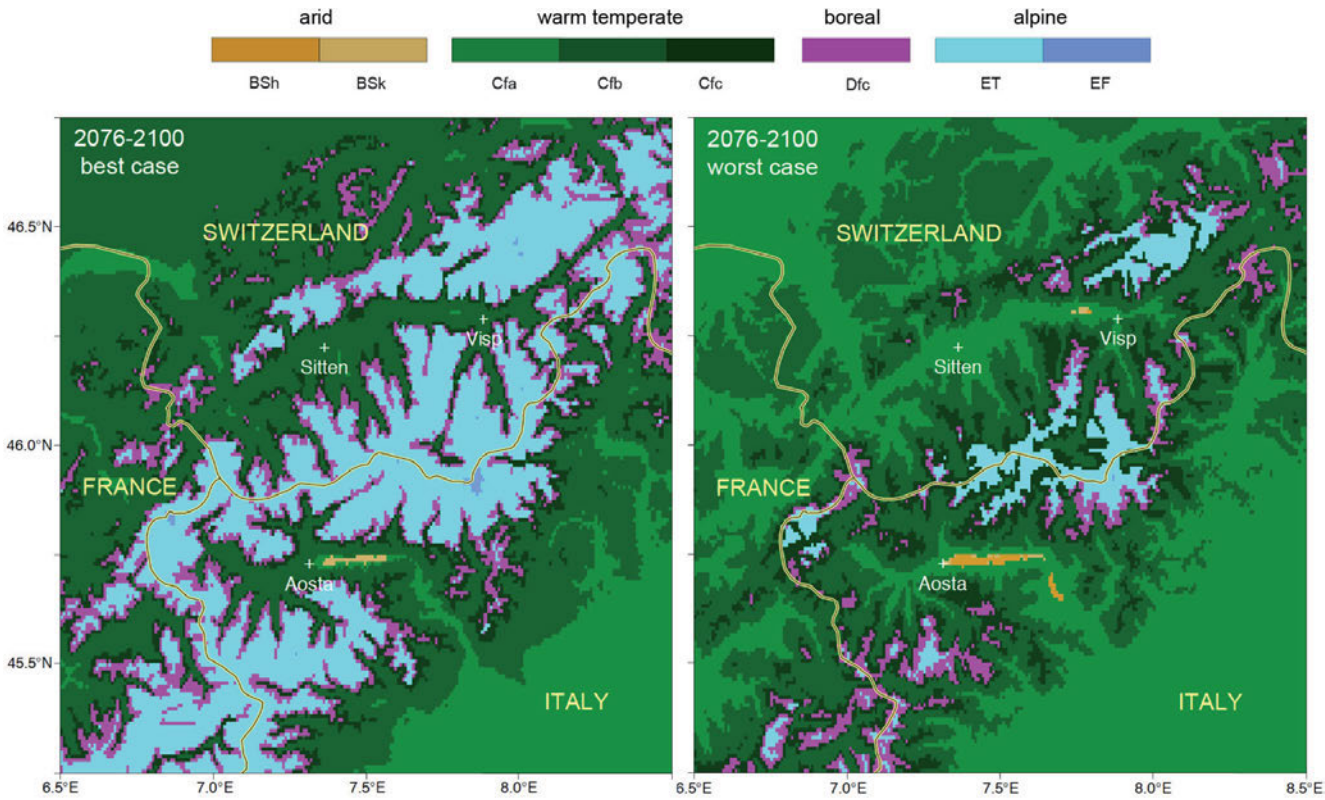

Figure 5: Köppen-Geiger climate maps for the Italian-Swiss-French border region depicting the inner Alpine dry valleys Wallis (with the cities Sitten and Visp) and Aosta. Rossby Centre regional atmospheric model RCA4 best case scenario RCP 2.6 (left) and worst case scenario RCP 8.5 (right). Period 2076–2100.

Further applications of the Köppen-Geiger maps may include the investigation of local effects such as the extension of inner Alpine dry valleys. These valleys are arid because they are located in the rain shadow of the Alpine divide. Fig. 5, a more detailed view of the projected climate maps for the period 2076–2100 (Fig. 2), depicts two well known dry valleys for which the Köppen-Geiger classification identifies dry steppe climate. The first is the Aosta valley in Northern Italy, the second the Wallis in Switzerland. While for the best case scenario, the cold steppe climate (BSk) was exclusively identified in the Aosta valley, for the worst case scenario both steppe climates, cold (BSk) and hot (BSh), were identified in the Wallis, as well as in the Aosta valley. Other well known inner Alpine dry valleys resolved by the very high resolution Köppen-Geiger maps are located in northern Italy and include the Veltlin, the Vinschgau and the Eisack valleys.

The studies discussed above demonstrate possible applications of the very high resolution climate maps. Users are invited to draw their own conclusions by applying the digital datasets to their region of interest. Particular advantage is expected for biological studies which are assessing the relationship between the abundance of plants, animals or pathogens to past, present and future climates. Many of these studies may also benefit from the printed maps, avoiding the more expensive application of the digital dataset.

Acknowledgments

We are grateful to Francesco Isotta and Christoph Frei, Federal Office of Meteorology and Climatology MeteoSwiss, Zurich, for providing high resolution gridded precipitation data, as well as Olaf Kahl for general editing and Clair Firth for English language editing.

References

Alvares, C.A., J.L. Stape, P.C. Sentelhas, J.L. de Moraes Goncalves, G. Sparovek, 2013: Köppen's climate classification map for Brazil. – Meteorol. Z. **22**, 711–728.

Auer, I., R. Böhm, A. Jurkovic, W. Lipa, A. Orlik, R. Potzmann, W. Schöner, M. Ungersböck, C. Matulla, K. Briffa, P. Jones, D. Efthymiadis, M. Brunetti, T. Nanni, M. Maugeri, L. Mercalli, O. Mestre, J.-M. Moisselin, M. Begert, G. Müller-Westermeier, V. Kveton, O. Bochnicek, P. Stastny, M. Lapin, S. Szalai, T. Szentimrey, T. Cegnar, M. Dolinar, M. Gajic-Capka, K. Zaninovic, Z. Majstorovic, E. Nieplova, 2007: HISTALP – historical instrumental climatological surface time series of the Greater Alpine Region. – Int. J. Climatol. **27**, 17–46.

Becker, A., P. Finger, A. Meyer-Christoffer, B. Rudolf, K. Schamm, U. Schneider, M. Ziese, 2013: A description of the global land-surface precipitation data products of the Global Precipitation Climatology Centre with sample applications including centennial (trend) analysis from 1901–present. – Earth Syst. Sci. Data **5**, 71–99.

Bellini, B.C., D. Zeppelini, 2008: Three new species of Seira Lubbock (Collembola, Entomobryidae) from Mataraca, Para'ba State, Brazil. – Zootaxa **1773**, 44–54.

Böhm, R., I. Auer, M. Brunetti, M. Maugeri, T. Nanni, W. Schöner, 2001: Regional temperature variability in the European Alps: 1760–1998 from homogenized instrumental time series. – Int. J. Climatol. **21**, 1779–1801.

Brugger, K., F. Rubel, 2013: Characterizing the species composition of European Culicoides vectors by means of the Köppen-Geiger climate classification. – Parasit. Vectors **6**, 333.

Chan, D., Q. Wu, G. Jiang, X. Dai, 2016: Projected shifts in Köppen climate zones over China and their temporal evolution in CMIP5 multi-model simulations. – Adv. Atmos. Sci. **33**, 283–293.

Chimani, B., C. Matulla, R. Böhm, M. Ganekind, 2011: Development of a longterm dataset of solid/liquid precipitation. – Adv. Sci. Res. **6**, 39–43.

Chimani, B., C. Matulla, R. Böhm, M. Hofstätter, 2013: A new high resolution absolute temperature grid for the Greater Alpine Region back to 1780. – Int. J. Climatol. **33**, 2129–2141.

Crosbie, R.S., D.W. Pollock, F.S. Mpelasoka, O.V. Barron, S.P. Charles, M.J. Donn, 2012: Changes in Köppen-Geiger climate types under a future climate for Australia: Hydrological implications. – Hydrol. Earth Syst. Sci. **16**, 3341–3349.

Diaz-Varela, R.A., R. Colombo, M. Meroni, M.S. Calvo-Iglesias, A. Buffonid, A. Tagliaferri, 2007: Spatio-temporal analysis of alpine ecotones: A spatial explicit model targeting altitudinal vegetation shifts. – Ecol. Mod. **221**, 621–633.

Efthymiadis, D., P.D. Jones, K.R. Briffa, I. Auer, R. Böhm, W. Schöner, C. Frei, J. Schmidli, 2006: Construction of a 10-min-gridded precipitation data set for the Greater Alpine Region for 1800–2003. – J. Geophys. Res. **111**, D01105.

Ellenberg, H., C. Leuschner, 2010: Vegetation Mitteleuropas mit den Alpen (Vegetation of Central Europe with the Alps, 6th edition). – Eugen Ulmer, Stuttgart, 1334pp.

Engelbrecht, C.J., F.A. Engelbrecht, 2014: Shifts in Köppen-Geiger climate zones over southern Africa in relation to key global temperature goals. – Theor. Appl. Climatol. **123**, 247–261.

Feng, S., Q. Hu, W. Huang, C.-H. Ho, R. Li, Z. Tang, 2014: Projected climate regime shift under future global warming from multi-model, multi-scenario CMIP5 simulations. – Global Planetary Change **112**, 41–52.

Fraedrich, K., F.-W. Gerstengarbe, P.C. Werner, 2001: Climate shift during the last century. – Climate Change **50**, 405–417.

Frei, C., C. Schär, 1998: A precipitation climatology of the Alps from high-resolution rain-gauge observations. – J. Climatol. **18**, 873–900.

Geiger, R., 1961: Überarbeitete Neuausgabe von Geiger, R.: Köppen-Geiger / Klima der Erde. (Wandkarte 1:16 Mill.) – Klett-Perthes, Gotha.

Gerstengarbe, F.-W., P. Hoffmann, H. Österle, P.C. Werner, 2015: Ensemble simulations for the RCP8.5-Scenario. – Meteorol. Z. **24**, 147–156.

Gottfried, M., M. Hantel, C. Maurer, R. Toechterle, H. Pauli, G. Grabherr, 2011: Climate effects on mountain plants. – Env. Res. Lett. **6**, 014013.

Grabherr, G., M. Gottfried, H. Pauli, 1994: Climate effects on mountain plants. – Nature **369**, 448–448.

Hantel, M., L.-M. Hirtl-Wielke, 2007: Sensitivity of Alpine snow cover to European temperature. – Int. J. Climatol. **27**, 1265–1275.

Hantel, M., C. Maurer, 2011: The median winter snowline in the Alps. – Meteorol. Z. **20**, 267–276.

Haslinger, K., W. Schöner, I. Anders, 2016: Future drought probabilities in the Greater Alpine Region based on COSMO-CLM experiments – spatial patterns and driving forces. – Meteorol. Z. **25**, 137–148.

Hijmans, R.J., S.E. Cameron, J.L. Parra, P.G. Jones, A. Jarvis, 2005: Very high resolution interpolated climate surfaces for global land areas. – Int. J. Climatol. **25**, 1965–1978.

Isotta, F.A., C. Frei, V. Weilguni, M.P. Tadić, P. Lassègues, B. Rudolf, V. Pavan, C. Cacciamani, G. Antolini, S.M. Ratto, M. Munari, S. Micheletti, V. Bonati, C. Lussana, C. Ronchi, E. Panettieri, G. Marigo, G. Vertačnik, 2014: The climate of daily precipitation in the Alps: development and analysis of a high-resolution grid dataset from pan-Alpine rain-gauge data. – Int. J. Climatol. **34**, 1657–1675.

Isotta, F.A., R. Vogel, C. Frei, 2015: Evaluation of European regional reanalyses and downscalings for precipitation in the Alpine region. – Meteorol. Z. **24**, 15–37.

Jacob, D., J. Petersen, B. Eggert, A. Alias, O.B. Christensen, L. Bouwer, A. Braun, A. Colette, M. Déqué, G. Georgievski, E. Georgopoulou, A. Gobiet, L. Menut, G. Nikulin, A. Haensler, N. Hempelmann, C. Jones, K. Keule, S. Kovats, N. Kröner, S. Kotlarski, A. Kriegsmann, E. Martin, E. Meijgaard, C. Moseley, S. Pfeifer, S. Preuschmann, C. Radermacher, K. Radtke, D. Rechid, M. Rounsevell, P. Samuelsson, S. Somot, J.-F. Soussana, C. Teichmann, R. Valentini, R.Vautard, B. Weber, P. Yiou, 2014: EURO-CORDEX: new high-resolution climate change projections for European impact research. – Reg. Env. Change **14**, 563–578.

Jobbágy, E.G., R.B. Jackson, 2000: Global controls of forest line elevation in the northern and southern hemispheres. – Global Ecol. Biogeogr. **9**, 253–268.

Köppen, W., 1919: Baumgrenze und Lufttemperatur (Timberline and air temperature). – Petermanns Geogr. Mitt. **65**, 201–203.

Köppen, W., 1920: Verhältnis der Baumgrenze zur Lufttemperatur (Relationship between timberline and air temperature). – Meteorol. Z. **37**, 39–42.

Köppen, W., 1936: Das geographische System der Klimate (The geographic system of climates). – In: Köppen, W., R. Geiger (Hrsg.): Handbuch der Klimatologie, Bd. 1, Teil C. – Borntraeger, Berlin, 44 pp.

Kotlarski, S., K. Keuler, O.B. Christensen, A. Colette, M. Déqué, A. Gobiet, K. Goergen, D. Jacob, D. Lüthi, van E. Meijgaard, G. Nikulin, C. Schär, C. Teichmann, R. Vautard, K. Warrach-Sagi, V. Wulfmeyer, 2014: Regional climate modeling on European scales: A joint standard evaluation of the EURO-CORDEX RCM ensemble. – Geosci. Model Dev. **7**, 1297–1333.

Kottek, M., J. Grieser, C. Beck, B. Rudolf, F. Rubel, 2006: World map of the Köppen-Geiger climate classification updated. – Meteorol. Z. **15**, 259–263.

Manabe, S., J.L. Holloway, 1975: The seasonal variation of the hydrologic cycle as simulated by a global model of the atmosphere. – J. Geophys. Res. **80**, 1617–1649.

Meinshausen, M., S.J. Smith, K. Calvin, J.S. Daniel, M.L.T. Kainuma, J.-F. Lamarque, K. Matsumoto, S.A. Montzka, S.C.B. Raper, K. Riahi, A. Thomson, G.J.M. Velders,, D.P.P. van Vuuren, 2011: The RCP greenhouse gas concentrations and their extensions from 1765 to 2300. – Climatic Change **109**, 213–241.

Mitchell, T.D., P.D. Jones, 2005: An improved method of constructing a database of monthly climate observations and associated high-resolution grids. – Int. J. Climatol. **25**, 693–712.

Mizoguchi, Y., A. Miyata, Y. Ohtani, R. Hirata, S. Yuta, 2009: A review of tower flux observation sites in Asia. – J. For. Res. **14**, 1–9.

Rodríguez Algeciras, J.A., L.G. Consuegra, A. Matzarakis, 2016: Spatial-temporal study on the effects of urban street configurations on human thermal comfort in the world heritage city of Camagüey-Cuba. – Building Env. **101**, 85–101.

Rolland, C., 2003: Spatial and seasonal variations of air temperature lapse rates in Alpine regions. – J. Climate **16**, 1032–1046.

Rubel, F., M. Kottek, 2010: Observed and projected climate shifts 1901–2100 depicted by world maps of the Köppen-Geiger climate classification. – Meteorol. Z. **19**, 135–141.

Rubel, F., M. Kottek, 2011: Comments on: 'The thermal zones of the Earth' by Wladimir Köppen (1884). – Meteorol. Z. **20**, 361–365.

Samuelsson, P., C.G. Jones, U. Willén, A. Ullerstig, S. Gollvik, U. Hansson, C. Jansson, E. Kjellström, G. Nikulin, K. Wyser, 2011: The Rossby Centre Regional Climate model RCA3: model description and performance. – Tellus **63A**, 4–23.

Santini, M., di A. Paola, 2015: Changes in the world rivers' discharge projected from an updated high resolution dataset of current and future climate zones. – J. Hydrol. **531**, 768–780.

Schneider, U., A. Becker, P. Finger, A. Meyer-Christoffer, M. Ziese, B. Rudolf, 2014: GPCC's new land surface precipitation climatology based on quality-controlled in situ data and its role in quantifying the global water cycle. – Theor. Appl. Climatol. **115**, 15–40.

Schwarb, M., C. Frei, C. Schär, C. Daly, 2000: Mean annual precipitation throughout the European Alps 1971–1990. In: Hydrological Atlas of Switzerland, Plates 2.6. – Federal Office for Water and Geology, Bern.

Shakesby, R.A., 2011: Post-wildfire soil erosion in the Mediterranean: Review and future research directions. – Earth-Sci. Rev. **105**, 71–100.

Strandberg, G., L. Bärring, U. Hansson, C. Jansson, C. Jones, E. Kjellström, M. Kolax, M. Kupiainen, G. Nikulin, P. Samuelsson, A. Ullerstig, S. Wang, 2014: CORDEX scenarios for Europe from the Rossby Centre regional climate model RCA4. – Report Meteor. Climatol. No. **116**, SMHI, Norrköping, Sweden.

Szerencsits, E., 2012: Swiss tree lines – a GIS-based approximation. – Landscape Online **28**, 1–18.

Theurillat, J.-P., A. Guisan, 2001: Potential impact of climate change on vegetation in the European Alps: A review. – Climatic Change **50**, 77–109.

Torma, C., F. Giorgi, E. Coppola, 2015: Added value of regional climate modeling over areas characterized by complex terrain – Precipitation over the Alps. – J. Geophys. Res. Atmos. **120**, 3957–3972.

Willmes, C., D. Becker, S. Brocks, C. Hütt, G. Bareth, 2016: High resolution Köppen-Geiger classifications of paleoclimate simulations. – Trans. in GIS, DOI:10.1111/tgis.12187.

Yoo, J., R.V. Rohli, 2016: Global distribution of Köppen-Geiger climate types during the Last Glacial Maximum, Mid-Holocene, and present. – Palaeogeogr. Palaeoclimatol. Palaeoecol. **446**, 326–337.

Zanobetti, A., J. Schwartz, 2009: The effect of fine and coarse particulate air pollution on mortality: A national analysis. – Env. Health Perspect. **117**, 898–903.

Zhang, C., D. Lu, X. Chen, Y. Zhang, B. Maisupova, Y. Tao, 2016a: The spatiotemporal patterns of vegetation coverage and biomass of the temperate deserts in Central Asia and their relationships with climate controls. – Remote Sens. Environ. **175**, 271–281.

Zhang, L., C. Wang, X. Li, K. Cao, Y. Song, B. Hu, D. Lu, Q. Wang, X. Du, S. Cao, 2016b: A new paleoclimate classification for deep time. – Palaeogeogr. Palaeoclimatol. Palaeoecol. **443**, 98–106.